

## Supplementary Information

### Microkinetic modelling and analysis of CO<sub>2</sub> methanation on Ruthenium

Aswathy K. Raghu, Niket S. Kaisare\*

Department of Chemical Engineering, Indian Institute of Technology Madras,  
Chennai 600036, India

\*Corresponding Author: [nkaisare@iitm.ac.in](mailto:nkaisare@iitm.ac.in); Phone: [+91] (44) 2257-4176

#### 1. MICROKINETIC MODEL

Table S.1: The microkinetic model, comprising of forward and backward reaction pairs, and the corresponding rate parameters. Pre-exponential factors are expressed in CGS units (cm, mol, s) and the site density is  $\Gamma = 2.623 \times 10^{-09}$  mol/cm<sup>2</sup>. †These activation energies were taken from DFT literature <sup>1,2</sup>.

No.	Reaction	$S_i$ or $A_i$	$\beta$	$E_i$ (kJ/mol)
1	CO <sub>2</sub> + * → CO <sub>2</sub> *	0.85		0.00
2	CO <sub>2</sub> * → CO <sub>2</sub> + *	1.000E+13		10.61
3	H <sub>2</sub> + * + * → H* + H*	0.25		0.00
4	H* + H* → H <sub>2</sub> + * + *	4.248E+23	-0.098	101.8
5	CH <sub>4</sub> * → CH <sub>4</sub> + *	1.000E+13		3.86
6	CH <sub>4</sub> + * → CH <sub>4</sub> *	0.073		0.00
7	H <sub>2</sub> O* → H <sub>2</sub> O + *	1.000E+13		20.26
8	H <sub>2</sub> O + * → H <sub>2</sub> O*	1.0		0.00
9	CO* → CO + *	6.964E+9	1.5292	-0.1282*T + 189.54
10	CO + * → CO*	0.8		0.00
11	CO <sub>2</sub> * + * → CO* + O*	3.812E+20		25.14
12	CO* + O* → CO <sub>2</sub> * + *	1.525E+22		73.78
13	CO <sub>2</sub> * + H* → COOH* + *	7.625E+20		96.48†
14	COOH* + * → CO <sub>2</sub> * + H*	1.525E+21		52.99
15	COOH* + * → CO* + OH*	1.525E+21		22.72
16	CO* + OH* → COOH* + *	7.625E+21		61.00
17	CO* + H* → COH* + *	1.525E+22		216.01
18	COH* + * → CO* + H*	3.431E+21		0.00
19	CO* + H* → HCO* + *	1.144E+22		153.12

20	$\text{HCO}^* + * \rightarrow \text{CO}^* + \text{H}^*$	3.812E+18		0.00
21	$\text{HCO}^* + * \rightarrow \text{CH}^* + \text{O}^*$	3.812E+21		91.15
22	$\text{CH}^* + \text{O}^* \rightarrow \text{HCO}^* + *$	3.812E+21		170.08
23	$\text{C}^* + \text{H}^* \rightarrow \text{CH}^* + *$	7.625E+21		64.28
24	$\text{CH}^* + * \rightarrow \text{C}^* + \text{H}^*$	2.287E+21		82.01 <sup>†</sup>
25	$\text{CH}^* + \text{H}^* \rightarrow \text{CH}_2^* + *$	3.812E+21		85.74
26	$\text{CH}_2^* + * \rightarrow \text{CH}^* + \text{H}^*$	2.287E+21		14.47 <sup>†</sup>
27	$\text{CH}_2^* + \text{H}^* \rightarrow \text{CH}_3^* + *$	3.812E+21		45.63
28	$\text{CH}_3^* + * \rightarrow \text{CH}_2^* + \text{H}^*$	1.906E+21		41.49 <sup>†</sup>
29	$\text{CH}_3^* + \text{H}^* \rightarrow \text{CH}_4^* + *$	1.525E+21		36.76
30	$\text{CH}_4^* + * \rightarrow \text{CH}_3^* + \text{H}^*$	7.625E+20		49.20 <sup>†</sup>
31	$\text{O}^* + \text{H}^* \rightarrow \text{OH}^* + *$	7.982E+27	-1.678	0.049*T + 83.986
32	$\text{OH}^* + * \rightarrow \text{O}^* + \text{H}^*$	2.004E+27	-1.6795	0.0486*T + 30.345
33	$\text{OH}^* + \text{H}^* \rightarrow \text{H}_2\text{O}^* + *$	1.838E+28	-2.4157	0.0592*T + 38.107
34	$\text{H}_2\text{O}^* + * \rightarrow \text{OH}^* + \text{H}^*$	1.837E+27	-2.4157	0.0592*T + 36.757
35	$\text{COH}^* + * \rightarrow \text{C}^* + \text{OH}^*$	6.176E+24		55.41
36	$\text{C}^* + \text{OH}^* \rightarrow \text{COH}^* + *$	7.625E+21		125.65
37	$\text{CO}_2^* + \text{H}^* \rightarrow \text{HCOO}^{**}$	3.812E+20		35.70 <sup>†</sup>
38	$\text{HCOO}^{**} \rightarrow \text{CO}_2^* + \text{H}^*$	1.00E+12		11.68
39	$\text{HCOO}^{**} \rightarrow \text{HCO}^* + \text{O}^*$	7.50E+13		103.79
40	$\text{HCO}^* + \text{O}^* \rightarrow \text{HCOO}^{**}$	3.812E+20		23.33
41	$\text{CO}^* + * \rightarrow \text{C}^* + \text{O}^*$	2.473E+28	-0.4494	0.2814*T + 23.766
42	$\text{C}^* + \text{O}^* \rightarrow \text{CO}^* + *$	2.825E+25	-0.4516	0.2813*T - 68.102

## 2. CHEMKIN INPUT FILE FOR 350 °C

The Chemkin input file at 350 °C is attached with this document. Since Chemkin does not support temperature dependent activation energies, the input file at one temperature is provided. For use at other temperatures, activation energies of the sensitive reactions may be calculated and replaced using the formulae given in Table S.1.

```

MATERIAL SABATIERMETH
SITE/RUTHENIUM/      SDEN/2.623E-9/
  (Ru) H2O (Ru) H (Ru) HCOO (Ru) /2/ OH (Ru) CO (Ru) C (Ru)
  CH3 (Ru) CH2 (Ru) CH (Ru) CH4 (Ru) O (Ru) CO2 (Ru)
  HCO (Ru) COH (Ru) COOH (Ru)
END
!*****
REACTIONS  KJOULES/MOLE  MWOFF
CO2 + (Ru) => CO2 (Ru)          0.850E00   0.000   0.000   !!
      STICK

```

CO2 (Ru) => CO2 + (Ru)	1.00E+13	0.000	10.61	!2!
H2 + (Ru) + (Ru) => H(Ru) + H(Ru)	0.250E00	0.000	0.000	!3!
STICK				
H(Ru) + H(Ru) => H2 + (Ru) + (Ru)	4.248E23	-0.0981	101.8	!4!
CH4 (Ru) => CH4 + (Ru)	1.00E+13	0.000	3.85	!5!
CH4 + (Ru) => CH4 (Ru)	7.300E-2	0.000	0	!6!
STICK				
H2O (Ru) => H2O + (Ru)	1.00E+13	0.000	20.26	!7!
H2O + (Ru) => H2O (Ru)	1.000E00	0.000	0	!8!
STICK				
CO (Ru) => CO + (Ru)	6.964E9	1.5292	109.65	!9!
CO + (Ru) => CO (Ru)	0.800E00	0.000	0	!10!
STICK				
CO2 (Ru) + (Ru) => CO (Ru) + O (Ru)	3.812E20	0.000	25.13	!11!
CO (Ru) + O (Ru) => CO2 (Ru) + (Ru)	1.525E22	0.000	73.77	!12!
CO2 (Ru) + H (Ru) => COOH (Ru) + (Ru)	7.625E20	0.000	96.48	!13!
COOH (Ru) + (Ru) => CO2 (Ru) + H (Ru)	1.525E21	0.000	52.98	!14!
COOH (Ru) + (Ru) => CO (Ru) + OH (Ru)	1.525E21	0.000	22.72	!15!
CO (Ru) + OH (Ru) => COOH (Ru) + (Ru)	7.625E21	0.000	61.001	!16!
CO (Ru) + H (Ru) => COH (Ru) + (Ru)	1.525E22	0.000	216.01	!17!
COH (Ru) + (Ru) => CO (Ru) + H (Ru)	3.431E21	0.000	0	!18!
CO (Ru) + H (Ru) => HCO (Ru) + (Ru)	1.144E22	0.000	153.12	!19!
HCO (Ru) + (Ru) => CO (Ru) + H (Ru)	3.812E18	0.000	0.00	!20!
HCO (Ru) + (Ru) => CH (Ru) + O (Ru)	3.812E21	0.000	91.15	!21!
CH (Ru) + O (Ru) => HCO (Ru) + (Ru)	3.812E21	0.000	170.08	!22!
C (Ru) + H (Ru) => CH (Ru) + (Ru)	7.625E21	0.000	64.27	!23!
CH (Ru) + (Ru) => C (Ru) + H (Ru)	2.287E21	0.000	82.008	!24!
CH (Ru) + H (Ru) => CH2 (Ru) + (Ru)	3.812E21	0.000	85.73	!25!
CH2 (Ru) + (Ru) => CH (Ru) + H (Ru)	2.287E21	0.000	14.47	!26!
CH2 (Ru) + H (Ru) => CH3 (Ru) + (Ru)	3.812E21	0.000	45.63	!27!
CH3 (Ru) + (Ru) => CH2 (Ru) + H (Ru)	1.906E21	0.000	41.48	!28!
CH3 (Ru) + H (Ru) => CH4 (Ru) + (Ru)	1.525E21	0.000	36.76	!29!
CH4 (Ru) + (Ru) => CH3 (Ru) + H (Ru)	7.625E20	0.000	49.20	!30!
O (Ru) + H (Ru) => OH (Ru) + (Ru)	7.982E27	-1.678	114.52	!31!
OH (Ru) + (Ru) => O (Ru) + H (Ru)	2.004E27	-1.6795	60.63	!32!
OH (Ru) + H (Ru) => H2O (Ru) + (Ru)	1.838E28	-2.4157	75.00	!33!
H2O (Ru) + (Ru) => OH (Ru) + H (Ru)	1.837E27	-2.4157	73.65	!34!
COH (Ru) + (Ru) => C (Ru) + OH (Ru)	6.176E24	0.000	55.41	!35!
C (Ru) + OH (Ru) => COH (Ru) + (Ru)	7.625E21	0.000	125.65	!36!
CO2 (Ru) + H (Ru) => HCOO (Ru)	3.812E20	0.000	35.69	!37!
HCOO (Ru) => CO2 (Ru) + H (Ru)	1.00E12	0.000	11.67	!38!
HCOO (Ru) => HCO (Ru) + O (Ru)	7.50E13	0.000	103.79	!39!
HCO (Ru) + O (Ru) => HCOO (Ru)	3.812E20	0.000	23.3	!40!
CO (Ru) + (Ru) => C (Ru) + O (Ru)	2.473E28	-0.4494	199.12	!41!
C (Ru) + O (Ru) => CO (Ru) + (Ru)	2.825E25	-0.4516	107.19	!42!

END

### 3. ADDITIONAL MODEL VALIDATIONS

#### 3.1. Equilibrium Conversion: The final model vs. the initial screening model

Prediction of equilibrium conversion calculated by Gao et al.<sup>3</sup> is compared to the predictions of our model and those of the model by Avanesian et al.<sup>1</sup> in Figure S.1. When the PFR is infinitely long, the system eventually reaches equilibrium. Hence, the simulations were run using the microkinetic model using a large value of reactor length to ensure equilibrium is attained at the corresponding temperature. The lines in Figure S.1 represent equilibrium conversion thus computed from the microkinetic models. The model by Avanesian et al.<sup>1</sup> is unable to predict the equilibrium conversion values.

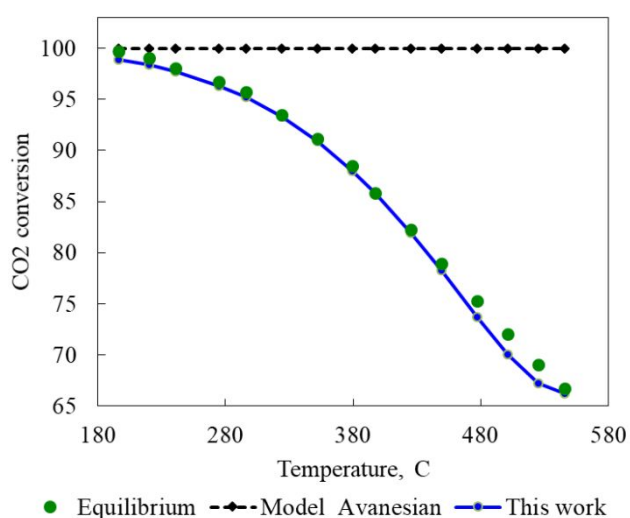


Figure S.1: Equilibrium conversion of CO<sub>2</sub>. The green dots represent the equilibrium conversion from Gao et al.<sup>3</sup>, the blue solid line indicates model predictions from the model in Table S.1, and the dashed black line indicates model predictions from the kinetic model from Avanesian et al.<sup>1</sup>.

#### 3.2. Case 5: Comparison with experimental results from Brooks et al.<sup>4</sup>

Brooks et al.<sup>4</sup> used 3% Ru-TiO<sub>2</sub> catalyst in a microreactor and performed experiments for a wide range of conditions. The PFR is 7 cm long with 1 mm diameter, and the residence times lie in the range 0.21 – 0.1 s. The feed comprises of 20% CO<sub>2</sub> and 80% H<sub>2</sub> and the surface area per unit length was fixed at  $a_l = 300$  cm. In addition to the CO<sub>2</sub> conversion, they also reported the inlet and outlet temperatures. The cases of near-isothermal operation reported in their work were simulated using our microkinetic model and are presented in Table S2. The comparison with experimental data shows that the model predicts the data qualitatively. However, it should be noted that the effect of support is not included in the model. Since the support TiO<sub>2</sub> is known to be active for the reaction<sup>4,5</sup>, our model which is developed without

considering the effect of support is expected to be inadequate. The reactor temperature is assumed to vary linearly between the inlet and outlet temperatures. When inlet and outlet temperatures are far apart, this assumption is a source of error and can cause deviation in prediction of conversion. Table shows that the model reasonably predicts their data.

Table S.2: A comparison between experimental data from Brooks et al. <sup>4</sup> and model predictions for various conditions.

No.	H <sub>2</sub> :CO <sub>2</sub>	T <sub>in</sub> (°C)	T <sub>out</sub> (°C)	U <sub>in</sub> (cm/s)	CO <sub>2</sub> conversion (%)	
					Experiments	Model
1	4	251	254	14.62	53.7	62.4
2	4	304	303	32.29	89.4	86.5
3	4	300	300	32.04	80.6	84.7
4	4	353	346	69.97	88.2	84.6
5	4	303	308	64.37	64	62.5
6	6	278	284	61.59	64	58.0

### 3.3. Comparison with CO methanation data

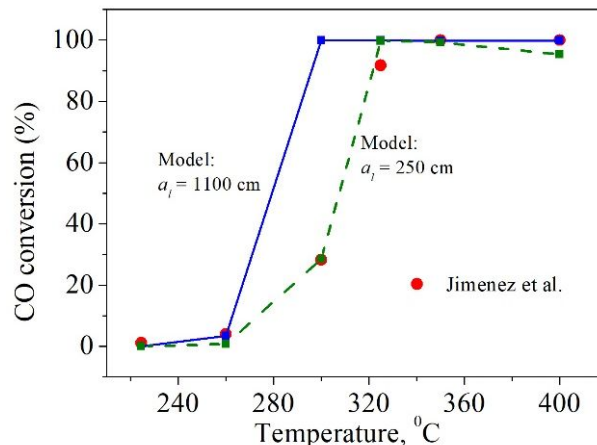


Figure S.2: Experimental data and model prediction of CO conversion vs. reactor temperature. Red dots represent experimental results from Jimenez et al. <sup>6</sup>, blue squares with solid line indicate model predictions when  $a_l = 1100$  cm and green circles connected by dashed line shows prediction with  $a_l = 250$  cm.

The microkinetic model was also checked for CO methanation since it is a similar reaction and likely to involve the same elementary steps. The experimental data is taken from Jimenez et al. <sup>6</sup> on 0.5 wt. % Ru on platelet carbon nanofiber catalyst and the comparison with model predictions is shown in Figure S.2. The area per unit length considered in CO<sub>2</sub> methanation for

Case-4 was  $a_l = 1100$  cm. With this value, the reaction occurred faster and approached equilibrium at lower temperatures (solid line in Figure S.2). However, when a lower value of  $a_l = 250$  cm was used, the model predictions are reasonable (dashed line). Jimenez et al. <sup>6</sup> have reported that CO methanation is sensitive to structure of catalyst support unlike CO<sub>2</sub> methanation and the microkinetic model is not designed to model the effect of support. Moreover, certain surface species such as CHOH\*, found to be relevant in CO methanation <sup>1,7</sup> is not included in the model.

#### 4. SENSITIVITY ANALYSIS

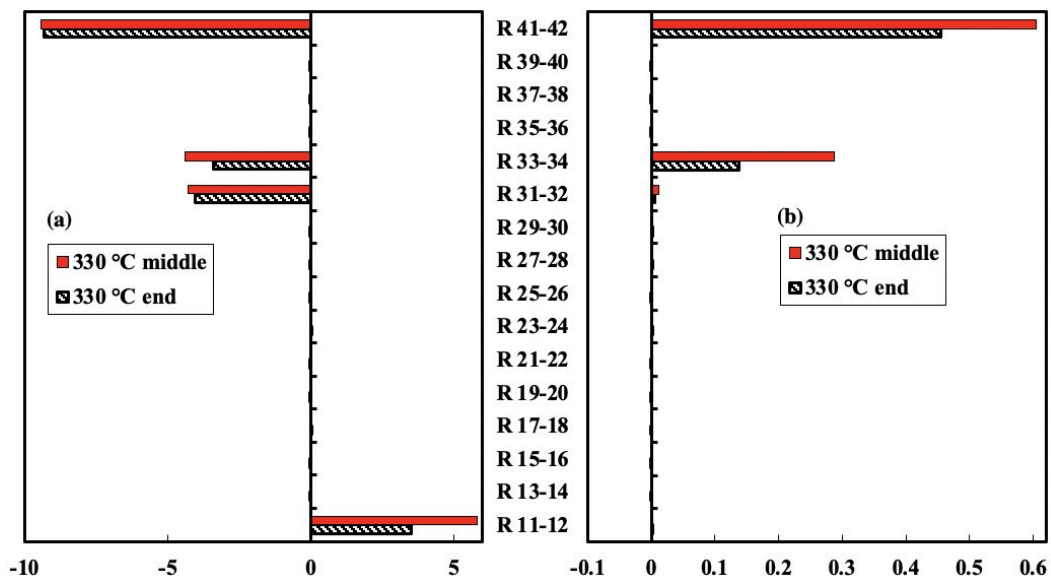


Figure S.3: Sensitivity analysis for the CH<sub>4</sub> mass fraction in the middle and end of the reactor, with respect to (a) activation energy, (b) pre-exponential factor.

Sensitivity analysis was performed by varying activation energies and pre-exponential factors and analyzing their effect on the CH<sub>4</sub> mass fraction at the middle and end of the fixed bed, with inlet conditions as those of Case 1 (for the experiments of Falbo et al.) and with temperature at 330 °C. Figure S.3 shows the pairwise brute-force sensitivity results for a 10% variation in activation energy (Figure S.3-a) and pre-exponential factor (Figure S.3-b). The rate constant for both forward and reverse reaction were varied simultaneously by the same amount and the following quantity was computed:

$$s = \frac{d \ln (Y_{\text{CH}_4})}{d \ln (\phi_i)} \approx \frac{\Delta Y_{\text{CH}_4} / Y_{\text{CH}_4}}{\Delta \phi_i / \phi_i}, \phi_i = A_{0i} \text{ or } E_i$$

The same reactions were found to be sensitive at both the locations. Note that the rate constants of the sensitive reactions, with the exception of R11-R12 pair, were the ones varied for fitting the experimental data, as described in Section 3.1 of the manuscript.

## REFERENCES

- (1) Avanesian, T.; Gusmao, G. S.; Christopher, P. Mechanism of CO<sub>2</sub> Reduction by H<sub>2</sub> on Ru(0 0 0 1) and General Selectivity Descriptors for Late-Transition Metal Catalysts. *J. Catal.* **2016**, *343*, 86–96. <https://doi.org/10.1016/j.jcat.2016.03.016>.
- (2) Zhang, S.-T.; Yan, H.; Wei, M.; Evans, D. G.; Duan, X. Hydrogenation Mechanism of Carbon Dioxide and Carbon Monoxide on Ru(0001) Surface: A Density Functional Theory Study. *RSC Adv.* **2014**, *4*, 30241–30249. <https://doi.org/10.1039/c4ra01655f>.
- (3) Gao, J.; Wang, Y.; Ping, Y.; Hu, D.; Xu, G.; Gu, F.; Su, F. A Thermodynamic Analysis of Methanation Reactions of Carbon Oxides for the Production of Synthetic Natural Gas. *RSC Adv.* **2012**, *2*, 2358–2368. <https://doi.org/10.1039/c2ra00632d>.
- (4) Brooks, K. P.; Hu, J.; Zhu, H.; Kee, R. J. Methanation of Carbon Dioxide by Hydrogen Reduction Using the Sabatier Process in Microchannel Reactors. *Chem. Eng. Sci.* **2007**, *62*, 1161–1170. <https://doi.org/10.1016/j.ces.2006.11.020>.
- (5) Hu, J.; Brooks, K. P.; Holladay, J. D.; Howe, D. T.; Simon, T. M. Catalyst Development for Microchannel Reactors for Martian in Situ Propellant Production. *Catal. Today* **2007**, *125* (1–2), 103–110. <https://doi.org/10.1016/j.cattod.2007.01.067>.
- (6) Jiménez, V.; Sánchez, P.; Panagiotopoulou, P.; Valverde, J. L.; Romero, A. Methanation of CO, CO<sub>2</sub> and Selective Methanation of CO, in Mixtures of CO and CO<sub>2</sub>, over Ruthenium Carbon Nanofibers Catalysts. *Appl. Catal. A Gen.* **2010**, *390*, 35–44. <https://doi.org/10.1016/j.apcata.2010.09.026>.
- (7) Loveless, B. T.; Buda, C.; Neurock, M.; Iglesia, E. CO Chemisorption and Dissociation at High Coverages during CO Hydrogenation on Ru Catalysts. *J. Am. Chem. Soc.* **2013**, *135*, 6107–6121. <https://doi.org/10.1021/ja311848e>.